Solvent Effect on the Global and Atomic DFT-Based Reactivity Descriptors Using the Effective Fragment Potential Model. Solvation of Ammonia

Robert Balawender,† Bennasser Safi, and Paul Geerlings*

Eenheid Algemene Chemie (ALGC), Faculteit Wetenschappen, Vrije Universiteit Brussel, Pleinlaan2, B-1050 Brussels, Belgium

Received: December 20, 2000

The effective fragment potential (EFP) model has been used to study the effect of adding increasing numbers of the water molecules on several DFT-based reactivity descriptors of NH_3. The HOMO−LUMO gap and electrophilic hardness are seen to increase with addition of water molecules. The importance on the wave function relaxation in the solvent effect on ammonia's properties is shown when analyzing the relaxation part in the electrophilic hardness and condensed Fukui function for the nitrogen atom. An increase in the atomic softness for the nitrogen atom with decreasing the global softness is observed. The saturation point for solvatation of ammonia was located around a cluster with 16 molecules of water. Atomic properties such as the Mulliken population, condensed Fukui function, and atomic softness for nitrogen and electrophilic global properties such as the hardness and its components for dilute solutions are predicted faithfully.

1. Introduction

A large part of chemistry and biochemistry occurs in solution, where the interaction of a large number of solvent molecules affects the structure and reactivity of the solute. Because of the size of the solute−solvent system, computational modeling is extremely difficult, and the vast majority of calculations is still performed with isolated solute molecules in the gas phase, generally a very poor model for solution chemistry. Solvation effects are most commonly included in ab initio calculations via continuum models,[1] but several methods have been proposed which include discrete solvent molecules.[2] In the discrete approach, solvent molecules are treated explicitly so that specific interactions between solute and solvent are taken into account. However, the size of the system increases dramatically with the number of solvent molecules, imposing computational limitations. In the dielectric continuum model, the most popular choice for describing solvents in the context of electronic structure theory, the solvent is described as an infinite, isotropic dielectric in which the solute is embedded. The recently introduced "effective fragment potential" (EFP) method belongs to the discrete solvent models.[3,4] In this method, one typically divides the total system into two parts, an active region treated ab initio and a fragment region. Then the fragment−fragment and/or fragment-active region interactions are calculated within the framework of the EFP methodology (see section 2.2). This method therefore seems to us a workable compromise of quality and cost. This model has been applied to the calculation of ribonuclease,[5] small water clusters,[6] formamide,[7,8] glutamic acid,[9] and water−sodium chloride clusters.[10] A combined EPF/Onsager model (discrete/continum model) has recently been used for the calculation of the relative stabilities of the neutral and zwitterionic forms of glycine.[11]

The intention of this work is to evaluate the influence of the solvent on reactivity, as represented by a series of reactivity descriptors which have been introduced or refined in recent years in within the context of conceptual density functional theory (DFT).[12−15] These descriptors both involve global properties (i.e., properties of a molecule as a whole) such as electronegativity (χ) and chemical potential (μ),[16] global hardness (η)[17] and global softness (S), and local reactivity descriptors, varying from point to point such as local softness ($s(\mathbf{r})$)[18], and the Fukui function ($f(\mathbf{r})$).[19] These concepts have been used extensively as such and within the context of principles such as the Pearson's hard and soft acids and bases principle,[20] Sanderson's electronegativity equalization principle,[21] and Parr and Pearson's maximum hardness[22] principle, for, e.g., discussing intramolecular reactivity trends (site selectivity).[23,24]

However, almost all of the calculations of these properties were performed in the gas phase. Recently, the computational scheme for functional group electronegativity, hardness, and softness[25] was extended to include the effect of a solvent using a continuum model;[26] the values obtained were used successfully in the study of the acidity of alkyl-substituted alcohols and the basicity of amines[26,27] and in an DFT-based interpretation of the solvent effect on the kinetic and thermodynamic aspects of the S_N2 reaction.[28] As a sequel to these studies, we present in this paper a first step to include the effects of solvent in a discrete appraoch, following the EFP model.[3,4]

In general, the EFP model treats each solvent molecule explicitly, by adding one-electron terms directly to the ab initio Hamiltonian

$$H_{\mathrm{TOT}} = H_{\mathrm{AR}} + V \tag{1}$$

where H_{AR} is the ab initio Hamiltonian describing the ''active region" of the system (solute and any solvent molecules that directly participate in bond making or breaking process)

$$V = V^{\mathrm{elec}} + V^{\mathrm{pol}} + V^{\mathrm{rep}} \tag{2}$$

The three one-electron terms in V, representing the potential due to the solvent (fragment) molecules, correspond to electrostatic, polarization, and exchange repulsion/charge-transfer

* Corresponding author. E-mail: pgeerlin@vub.ac.be.
† Permanent address: Institute of Physical and Theoretical Chemistry, Wrocław University of Technology, Wyb. Wyspiańskiego 27, Pl-50-370 Wrocław, Poland.

10.1021/jp0045538 CCC: $20.00
Published on Web 06/19/2001

interactions between the solvent molecules and the electrons and nuclei in the active region, as well as solvent−solvent interactions. There are no exchange repulsion/charge transfer terms in the nuclear−solvent interaction. The solute (including the desired number of solvent molecules) is explicitly treated with the ab initio wave function of choice, while effective fragments represent the solvent.

The present work reports a systematic study of solvent effects (in casu water) on the reactivity, as measured by its global and atomic descriptors, on a single system NH_3, serving as a case study to prepare a systematic investigation on a large series of small molecules.[29] We thereby explore both methodological and physical aspects. The basic approach is the combination of the EFP model and the CPHF approach,[30] the former in order to avoid the finite difference technique problems[12,26,31] when evaluating DFT-based reactivity descriptors. This technique has been recently developed by us[30] and successfully applied to the calculation of the nuclear Fukui function for a series of diatomics and the study of the Jahn Teller effect.[32,33]

2. Theoretical Background

2.1. DFT Reactivity Descriptors in the Gas Phase: the CPHF Approach. Global and local reactivity descriptors in DFT

$$\chi = -\mu = -\left(\frac{\partial E}{\partial N}\right)_{v(\mathbf{r})} \tag{3}$$

$$\eta = \frac{1}{2}\left(\frac{\partial^2 E}{\partial N^2}\right)_{v(\mathbf{r})} = \frac{1}{2}\left(\frac{\partial \mu}{\partial N}\right)_{v(\mathbf{r})} \tag{4}$$

$$S = \left(\frac{\partial N}{\partial \mu}\right)_{v(\mathbf{r})} = \frac{1}{2\eta} \tag{5}$$

and

$$f(\mathbf{r}) = \left(\frac{\partial \rho(\mathbf{r})}{\partial N}\right)_{v(\mathbf{r})} \tag{6}$$

$$S(\mathbf{r}) = f(\mathbf{r})S \tag{7}$$

are typically derivatives with respect to the total number of electrons at constant external potential ("frozen" geometry of the molecule), $(\partial/\partial N)_{v(\mathbf{r})}$.[14] The derivatives at some integral value N_o will in general have different values at the right-hand ($N_o + \delta$, electron inflow, chemical reduction) and left-hand ($N_o - \delta$, electron outflow, chemical oxidation) sides. Their average indicates reactivity toward a radical reagent. The coupled perturbed Hartree−Fock approach, presented in ref 30, has been used instead of the "popular" finite difference approach.[12,26,31] From the chain rule, we have

$$\left(\frac{\partial}{\partial N}\right)_{v(\mathbf{r})} = \left(\frac{\partial}{\partial \mathbf{n}}\right)_{v(\mathbf{r}),\mathbf{C}}\left(\frac{\partial \mathbf{n}}{\partial N}\right)_{v(\mathbf{r})} + \left(\frac{\partial}{\partial \mathbf{C}}\right)_{v(\mathbf{r}),\mathbf{n}}\left(\frac{\partial \mathbf{C}}{\partial N}\right)_{v(\mathbf{r})} \tag{8}$$

where the **n** diagonal matrix contains the MO occupations (2 for occupied MO and 0 for virtual MO) and **C** is the wave function coefficients matrix. For canonical orbitals and under condition that only the highest occupied (HO) and lowest unoccupied (LU) MO are involved during electron displacements, the **f** matrix defined as $\mathbf{f} = (\partial \mathbf{n}/\partial N)_{v(\mathbf{r})}$ has the form

$$f_i^{\pm} = \begin{cases} 1 \text{ for } i = \text{LUMO/HOMO} \\ 0 \text{ for } i \neq \text{LUMO/HOMO} \end{cases} \tag{9}$$

Within the CPHF approach and concentrating on the restricted Hartree−Fock (RHF) theory, the derivative of the μth coefficient of the ith MO with respect to N may be expanded in the basis of unchanged MOs[30,32]

$$\left(\frac{\partial c_{\mu i}}{\partial N}\right)_{v(\mathbf{r})} = \sum_k^{\text{MO}} c_{\mu k} U_{ki}^{\lambda} \qquad \text{or} \qquad \left(\frac{\partial \mathbf{C}}{\partial N}\right)_{v(\mathbf{r})} = \mathbf{CU} \tag{10}$$

where the **U** matrix element is equal (i virtual and j occupied orbital, FMO = frontier molecular orbital)

$$U_{ij}^{\pm} = \sum_k^{\text{vir}}\sum_l^{\text{occ}} A_{ij,kl}^{-1}\left((kl|\text{FMO,FMO}) - \frac{1}{2}(k,\text{FMO}|\text{l,FMO})\right) \tag{11}$$

and $(ij|kl)$ stands for a two-electron repulsion integral in MO basis.

The symmetrical **A** matrix is defined as

$$A_{ij,kl} = \delta_{ij,kl}(e_i - e_j) - 4(ij|kl) + (ik|jl) + (il|jk) \tag{12}$$

Electronegativity, the first derivative of the energy with respect to n, can be written as

$$\mu^{\pm} = \left(\frac{\partial E}{\partial N}\right)_{v(\mathbf{r})}^{\pm} = e_{\text{LUMO|HOMO}} \tag{13}$$

where e_{HOMO} and e_{LUMO} are frontier orbital energies. The global hardness, the second derivative of the energy, is thereby expressed as

$$\eta = \frac{1}{2}\left(\frac{\partial \mu}{\partial N}\right)_{v(\mathbf{r})} = \frac{1}{4}J_{\text{FMO}} + \sum_i^{\text{vir}}\sum_j^{\text{occ}} U_{ij}[2(i,j|\text{FMO,FMO}) - (i,\text{FMO}|j,\text{FMO})] \tag{14}$$

$J_{\text{FMO}} = (\text{FMO,FMO}|\text{FMO,FMO})$ is the Coulomb integral for the frontier orbital (FMO).

The condensed version of the local Fukui function ($f(\mathbf{r}) = (\partial\rho(\mathbf{r})/\partial N)_{v(\mathbf{r})}$ for atom A, given by the derivative of the Mulliken atomic population, can be written as

$$\left(\frac{\partial n_A}{\partial N}\right)_{v(\mathbf{r})}^{\pm} = f_A^{f\pm} + f_A^{U\pm} = f_A^{\pm} \tag{15}$$

where $f_A^{f\pm} = \sum_{\mu\in A}^{\text{AO}}\sum_{\nu}^{\text{AO}} c_{\text{FMO}\mu}c_{\text{FMO}\nu}S_{\mu\nu}$ and $f_A^{U\pm} = 2\sum_k^{\text{vir}}\sum_i^{\text{occ}}U_{ki}^{\alpha}\sum_{\mu\in A}^{\text{AO}}\sum_{\nu}^{\text{AO}}(c_{k\mu}c_{i\nu} + c_{i\mu}c_{k\nu})S_{\mu\nu}$.

$S_{\mu\nu}$ represents the elements of the overlap matrix. f_A^f accounts for the effect of changing only MO occupations. The second term f_A^U represents the MO relaxation contribution for the frozen MO occupations. The contributions from the occupied−occupied and virtual−virtual orbital interactions vanish due to the antisymmetric property of the **U** matrix ($\mathbf{U}^{\text{T}} = -\mathbf{U}$).

Another local property, local softness ($s(\mathbf{r}) = [\delta N/\delta\rho(\mathbf{r})]_{v(\mathbf{r})} = f(\mathbf{r})S$, where $S = {}^1/_2\eta$ is the global softness), in its condensed version, atomic softness, can be calculated as

$$s_A^{\pm} = f_A^{\pm}S^{\pm} \tag{16}$$

Hereby however, we have to differentiate between average value of the softness in the form $\tilde{s}_A = {}^1/_2(s_A^+ - s_A^-)$ and as $s_A^0 = f_A^0S^0$ (their difference being ${}^1/_4(f_A^-S^+ + f_A^+S^-)$).

Equations 11−15 permit evaluating the DFT-based reactivity descriptors within the CPHF scheme. Note that the use of a non DFT calculation technique is not contradictory with the use of DFT-based reactivity descriptors.[14]

2.2. Inclusion of the Solvent Effect: the Effective Fragment Potential Method. To incorporate the EFP model into our calculation, we modified the Fock matrix to include the contribution from effective fragments by making the substitution of the **V** matrix

$$\mathbf{F} = \mathbf{H} + \mathbf{G} + \mathbf{V} \tag{17}$$

where **H** and **G** stand for one- and two-electron integrals matrix in MO basis, respectively.

The **V** matrix is the operator for the interaction between the fragment and the electron density matrix (V^{ef} operator for the interaction fragment−electron density)

$$\mathbf{V} = \mathbf{C}^{T}\mathbf{V}^{ef}\mathbf{C} \tag{18}$$

The additional term in the Fock matrix changes the geometry of the solute, which affects the atomic orbital integrals and the wave function coefficients. There is also an additional contribution from the interaction between solvent (in casu water) fragments and the solute molecule electron density. The chemical potential, eq 13, is then written as

$$\mu^{\pm} = e^{sol}_{FMO} = H^{sol}_{FMO} = G^{sol}_{FMO} + V^{sol}_{FMO} \tag{19}$$

Differences in the hardness value find their origin in the change in the AO integrals and the **C** and **U** matrices. But there is no direct contribution from the **V** matrix, as we have, in the chemical potential case. The Fukui function in the solvent changes as compared to that in the gas phase by differences in the **C** and **U** matrices. There is also a contribution from the change in the geometry as compared to that in the gas phase, which is expressed directly in the difference of the overlap matrix in the solvent.

3. Computational Details

NH_3 was treated at the restricted HF level of theory with a DZP(+) basis set,[34] while the surrounding water molecules were represented by the EFP method described above. Their number was progressively increased (see section 4), and for each NH_3-$(H2O)_n$ cluster, we have generated 80 starting structures. Around the NH_3 molecule, we have constructed a grid (with the distance between the grid's nodes equal to 2.2 Å). From 1.5*n* to 2*n* (*n* being the number of water fragments; e.g., for $n = 6$, 12 fragments, and for $n = 10$, 15 water molecules), nodes close to NH_3 were used for construction of the random starting structure. For all structures, we have performed a two-step geometry optimization using GAMESS, with options POSITION=EFOPT in the $EFRAG mode (if the fragment gradient is large, up to five geometry steps in which only the fragments move may occur, before the geometry of the ab initio piece is relaxed) and with the gradient convergence tolerance equal 10^{-7} Hartee/Bohr. After this, we took up to around 20 lowest-energy structures (depending on the order of magnitude of the energy differences when adding more isomers to the selection) and performed full geometry optimizations. The effective fragment potential has been incorporated within the GAMESS suite of programs.[35] The EFP model uses a rigid-body approximation. The internal coordinates of the fragments are fixed at their experimental values (OH bond = 0.944 Å and HOH angle = 106.70°), while the positions of the fragments relative to the solute or each other are fully optimized.

4. Results and Discussion

In the theoretical analysis of solvent effects, a problem of fundamental importance is the manner in which the electronic and molecular structure of an electrolyte is modified by placing it in contact with a polar solvent. It is not clear how the system progresses from a gas-phase molecule to dissociated ions as solvent molecules are added. Also, the fact that the number of local minima on the potential energy surface increases rapidly with increasing number of water fragments and the absence of an analytic Hessian prompted us to use only an average value of a given property for a given number of water molecules when analyzing global and atomic properties. Note that in Table 1, (arithmetic) average values are given (no Boltzmann average was aimed at in view of the $T = 0$ in the calculations). The number of water molecules in each complex considered and

TABLE 1: Total Energy for NH_3 in Gas Phase (kcal/mol), Number of Isomers *n* Considered in the $NH_3(H_2O)_n$ Complex Incremental Binding Energies (IBE, in kcal/mol), Energies of HOMO and LUMO Orbitals (e_{HOMO} and e_{LUMO}), Average Value of the Chemical Potential μ^0, and the HOMO−LUMO Energy Gap $\Delta_{HL}/2$ (in eV)[a]

n	no. of isomers	IBE	e_{HOMO}	e_{LUMO}	μ^0	$\Delta_{HL}/2$
0	1	−35271.99[b]	−11.436	6.128	−2.654	8.782
1	1	−6.96	−12.417	5.672	−3.372	9.045
2	2	−7.48	−12.138	6.020	−3.059	9.079
3	6	−9.92	−12.101	6.269	−2.916	9.185
4	13	−8.43	−12.115	6.319	−2.898	9.217
5	14	−8.95	−12.171	6.267	−2.952	9.219
6	14	−7.92	−11.965	6.658	−2.654	9.311
7	14	−11.94	−11.941	6.709	−2.616	9.325
8	12	−11.29	−11.978	6.727	−2.625	9.353
9	14	−11.12	−11.894	6.769	−2.562	9.331
10	23	−7.18	−11.929	6.835	−2.547	9.382
12	15	−7.96	−11.906	6.909	−2.499	9.408
14	16	−9.97	−11.969	6.862	−2.553	9.416
16	19	−10.13	−11.985	7.012	−2.486	9.498
18	14	−9.96	−11.940	7.116	−2.412	9.528
20	16	−9.90	−12.108	6.966	−2.571	9.537
25	17	−9.56	−11.944	7.117	−2.414	9.530
30	17	−9.89	−12.142	6.928	−2.607	9.535
35	14	−10.63	−12.073	7.021	−2.526	9.547
40	12	−11.34	−12.170	6.767	−2.701	9.468
45	17	−8.93	−12.199	6.785	−2.707	9.492
49	22	−9.57	−12.113	6.888	−2.612	9.500

[a] The NH_3 isolated gas-phase molecule values are given for comparison. [b] Total energy for NH_3 in the gas phase (kcal/mol).

TABLE 2: Value of Hardness and Their Components as a Function of the Number of Water Molecules Included (*n*) (all in eV)

n	η^{f-}	η^{U-}	η^{-}	η^{f+}	η^{U+}	η^{+}
0	4.308	−1.798	2.510	1.946	−0.180	1.766
1	4.274	−1.759	2.515	1.945	−0.179	1.766
2	4.267	−1.749	2.519	1.963	−0.185	1.778
3	4.250	−1.723	2.527	2.005	−0.198	1.807
4	4.246	−1.718	2.529	2.011	−0.200	1.811
5	4.250	−1.722	2.527	1.996	−0.195	1.801
6	4.238	−1.703	2.535	2.040	−0.210	1.830
7	4.239	−1.705	2.534	2.021	−0.204	1.817
8	4.234	−1.698	2.536	2.041	−0.211	1.831
9	4.241	−1.705	2.536	2.028	−0.206	1.821
10	4.234	−1.696	2.538	2.036	−0.209	1.827
12	4.232	−1.692	2.540	2.020	−0.204	1.816
14	4.234	−1.692	2.541	2.020	−0.203	1.817
16	4.231	−1.685	2.546	1.997	−0.195	1.802
18	4.230	−1.682	2.548	2.002	−0.196	1.806
20	4.233	−1.684	2.549	1.993	−0.193	1.800
25	4.232	−1.685	2.547	1.979	−0.189	1.790
30	4.230	−1.681	2.549	2.009	−0.198	1.811
35	4.233	−1.684	2.550	1.985	−0.191	1.794
40	4.236	−1.692	2.544	2.006	−0.198	1.808
45	4.236	−1.690	2.546	2.009	−0.199	1.810
49	4.237	−1.691	2.546	1.991	−0.193	1.799

TABLE 3: Mulliken Population (q^{Mull}), Nitrogen's Condensed Fukui Functions (f^-, f^+) and Their Components (f^{f-}, f^{U-}, f^{f+}, f^{U+}), and Atomic Softness (s^-, s^+, s^A, s^o, in 10*eV^{-1}) as a Function of the Number of Water Molecules Included (n)

n	q^{Mull}	f^{f-}	f^{U-}	f^-	f^{f+}	f^{U+}	f^+	s^-	s^+	s^A	s^0
0	7.747	0.959	−0.510	0.449	−0.288	−0.074	−0.363	0.895	−1.027	−0.066	0.209
1	7.800	0.958	−0.492	0.466	−0.290	−0.069	−0.358	0.927	−1.015	−0.044	0.260
2	7.816	0.958	−0.485	0.473	−0.284	−0.066	−0.350	0.939	−0.984	−0.022	0.296
3	7.867	0.959	−0.466	0.493	−0.272	−0.056	−0.328	0.975	−0.909	0.033	0.390
4	7.878	0.958	−0.462	0.497	−0.271	−0.054	−0.325	0.982	−0.898	0.042	0.406
5	7.869	0.958	−0.465	0.493	−0.275	−0.057	−0.332	0.975	−0.923	0.026	0.381
6	7.909	0.958	−0.449	0.509	−0.265	−0.050	−0.315	1.004	−0.861	0.071	0.456
7	7.901	0.959	−0.452	0.506	−0.269	−0.053	−0.322	0.999	−0.886	0.057	0.436
8	7.915	0.958	−0.447	0.511	−0.265	−0.050	−0.315	1.008	−0.861	0.073	0.461
9	7.906	0.958	−0.450	0.509	−0.269	−0.051	−0.320	1.003	−0.880	0.062	0.444
10	7.918	0.959	−0.445	0.514	−0.266	−0.050	−0.316	1.013	−0.866	0.074	0.466
12	7.923	0.959	−0.443	0.516	−0.268	−0.051	−0.319	1.016	−0.878	0.069	0.465
14	7.931	0.958	−0.440	0.519	−0.269	−0.048	−0.318	1.020	−0.874	0.073	0.474
16	7.943	0.958	−0.434	0.525	−0.273	−0.048	−0.321	1.030	−0.892	0.069	0.482
18	7.955	0.958	−0.429	0.529	−0.272	−0.046	−0.318	1.038	−0.883	0.078	0.498
20	7.953	0.958	−0.430	0.528	−0.275	−0.047	−0.322	1.036	−0.894	0.071	0.489
25	7.943	0.958	−0.433	0.525	−0.276	−0.049	−0.325	1.031	−0.908	0.061	0.476
30	7.959	0.958	−0.428	0.530	−0.272	−0.045	−0.317	1.040	−0.875	0.082	0.504
35	7.954	0.958	−0.429	0.529	−0.276	−0.047	−0.323	1.038	−0.901	0.068	0.488
40	7.930	0.958	−0.439	0.519	−0.272	−0.049	−0.322	1.020	−0.890	0.065	0.467
45	7.939	0.958	−0.435	0.523	−0.273	−0.047	−0.321	1.026	−0.886	0.070	0.477
49	7.936	0.958	−0.436	0.521	−0.277	−0.049	−0.325	1.024	−0.905	0.060	0.465

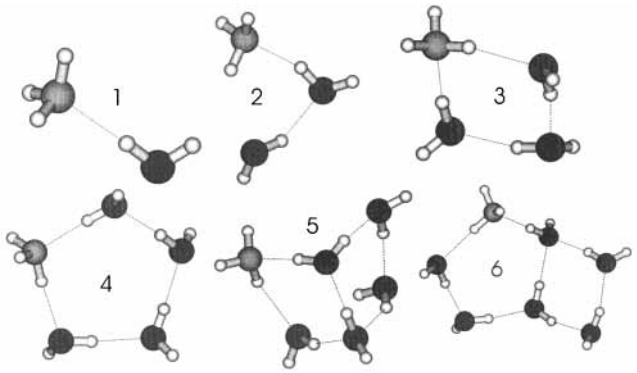

Figure 1. Structure for the lowest isomers for $NH_3(H_2O)_n$, $n = 1, 2, 3, 4, 5, 6$.

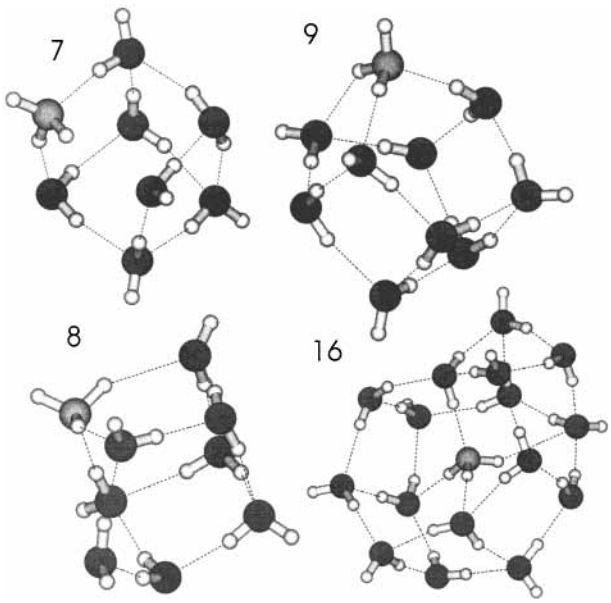

Figure 2. Structure for the lowest isomers for $NH_3(H_2O)_n$, $n = 7, 8, 9, 16$.

the number of isomers retained are given in Table 1. Computed global properties such as the chemical potential and hardness are listed in Tables 1 and 2. Atomic reactivity indices (Fukui function and atomic softness and Mulliken populations) are contained in Table 3.

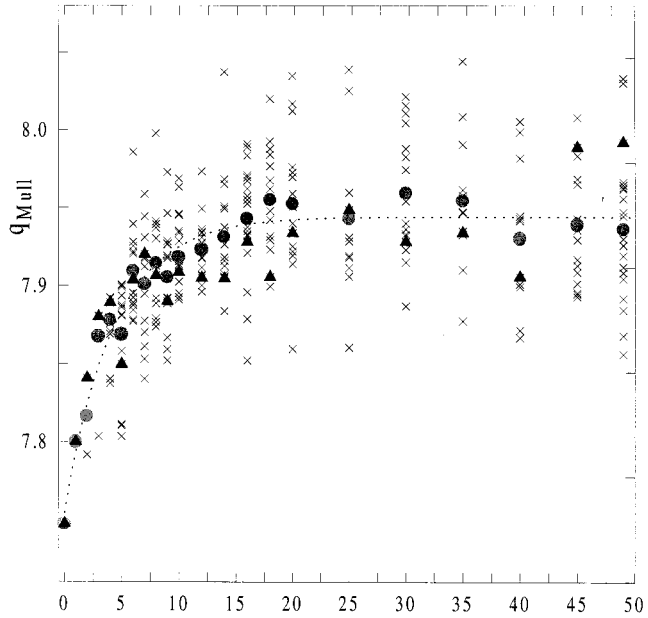

Figure 3. Mulliken population for nitrogen atom in $NH_3(H_2O)_n$ as a function of the number of water molecules, n. Crosses denote the values for the equilibrium geometries, triangles for the values of lowest-energy geometry, and circles for the average values.

In the third column in Table 1, we have listed the energy of NH_3 in gas phase and the incremental biding energy (IBE), defined as

$$\Delta E_{n-k,n} = (E_n - E_{n-k})/k \tag{20}$$

for the reaction $NH_3(H_2O)_{n-k} + kH_2O \rightarrow NH_3(H_2O)_n$ (k in general $\neq 1$ in order to account for the data in Table 1). We can see that value of the IBD is decreasing until $n = 7$, where it has its global minimum close to −12 kcal/mol; for $n = 10$, a local maximum is reached, and from $n = 14$, the value stabilizes at around −10 kcal/mol. The lowest energy structures for $n = 1-9$ and 16 are shown in Figures 1 and 2. The lowest-energy isomers for the smaller water clusters ($n \leq 4$) are found to be

TABLE 4: Atomic Properties of the N Atom and Global Properties for NH_3 in $NH_3(H_2O)_n$

	a	*b*	*c*	$n = 0$	$n = \infty$	R^2
			atomic properties for nitrogen atom in $NH_3(H_2O)_n$			
q^{Mull}	0.1896 ± 0.0090	−0.2294 ± 0.0223	7.7547 ± 0.0088	7.7474	7.9443 ± 0.0178	0.9641
f^{U-}	0.0743 ± 0.0034	−0.2078 ± 0.0199	−0.5073 ± 0.0034	−0.5096	−0.4331 ± 0.0068	0.9657
f^{-}	0.0740 ± 0.0034	−0.2090 ± 0.0201	0.4512 ± 0.0033	0.4494	0.5252 ± 0.0068	0.9655
s^{-}	0.1323 ± 0.0061	−0.2195 ± 0.0209	0.8983 ± 0.0060	0.8954	1.0306 ± 0.0121	0.9656
			global properties for in $NH_3(H_2O)_n$			
e_{LUMO}	1.1991 ± 0.1205	−0.1766 ± 0.0383	5.7790 ± 0.1177	6.1276	6.9781 ± 0.2382	0.8518
μ^o	1.1084 ± 0.1581	−0.3265 ± 0.0677	−3.6554 ± 0.1635	−2.6542	−2.5470 ± 0.3217	0.8585
$\Delta_{HL}/2$	0.6491 ± 0.0317	−0.1820 ± 0.0190	8.8632 ± 0.0310	8.7818	9.5123 ± 0.0626	0.9608
η^{f-}	−0.0712 ± 0.0032	−0.4235 ± 0.0379	4.3049 ± 0.0032	4.3076	4.2337 ± 0.0064	0.9679
η^{U-}	0.1046 ± 0.0047	−0.2852 ± 0.0258	−1.7921 ± 0.0047	−1.7981	−1.6874 ± 0.0094	0.9676
η^{f-}	0.0375 ± 0.0016	−0.1508 ± 0.0148	2.5102 ± 0.0016	2.5096	2.5477 ± 0.0032	0.9676

[a] Parameters *a*, *b*, and *c* and the standard errors for the nonlinear regression, eq 20, together with the calculated values in the gas phase ($n = 0$) and the predicted value and errors for the saturated system ($n = \infty$).

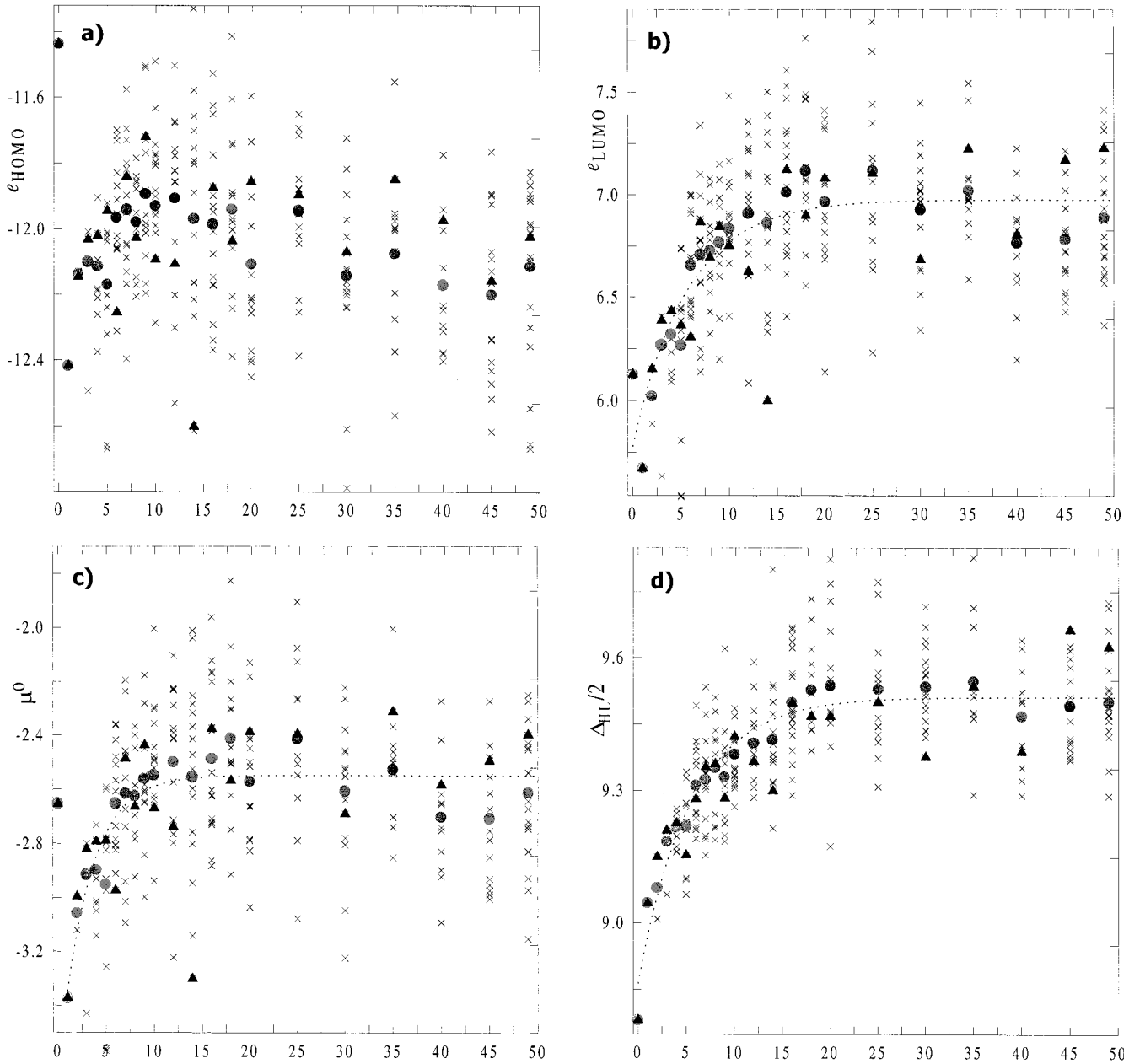

Figure 4. Global properties of $NH_3(H_2O)_n$ as a function of the number of water molecules, *n*; (a) energy of HO orbital, e_{HOMO}; (b) energy of LU orbital, e_{LUMO}; (c) average chemical potential, $\mu°$; (d) energy gap between HO and LU orbitals, $\Delta_{HL}/2$, (all in eV). See Figure 3 for details.

monocyclic, with each water monomer and ammonia participating as a single hydrogen-bond donor and acceptor. The all-lowest isomers for $n \leq 4$ have the nitrogen and oxygen atoms deviating very little from a common plane. Starting from $n = 6$, the structure of the lowest isomers are multiple rings. We can see from Figures 1 and 2 that the IBD has its minimum for

$n = 7$ due to the fact that the cluster has enough water molecules to form a cubic arrangement which maximizes the number of O···HO hydrogen bonds and minimizes their deviation from an ideal linear orientation (energetically favorable). Adding one more water molecules to the to $NH_3(H_2O)_7$ cluster enables the system to form a three-dimensional structure in which ammonia is in a five membered ring and each monomer acts as a triple hydrogen-bond donor or acceptor. The lowest-energy cluster with nine water molecules has a "sandwich" structure built from two five-membered rings, which is favorable for a $(H_2O)_5$ cluster and for ammonia with four water molecules. Until now, the ammonia molecule turns always out to be located in the corner of the structure; then additional water molecules start to close the shell around NH_3, and starting from $n = 16$, we can see in Figure 2 that ammonia is placed in the center of cluster with four hydrogen bonds, with the IBD stabilizing at around −10 kcal/mol.

Ammonia act as a Brønsted base because it readily accepts protons, and as Lewis base, as it behave as an electron-pair donor. When ammonia dissolves in water, only about 1% reacts to form ammonium and hydroxide ions; the remainder is present as unreacted NH_3 molecules. It can display acidic behavior although it is a much weaker acid than water. It reacts with very strong bases, such as the CH_3 anion. In this part, we will only analyze the left-side derivatives, which are associated with the essentially basic properties of ammonia; the right-side derivative (nucleophilic properties) will be only listed.

The fact that ammonia's hydrogens form a hydrogen bond with water's oxygen increases the Mulliken population on its nitrogen atom (as is well-known from detailed charge analysis of H-bond complexes[36] using Gutman's pile-up and spillover effects[37]). In Figure 3, we show the Mulliken population as a function of the number of water molecules included in cluster. To find the nitrogen's population for the saturated systems, we made a nonlinear regression of the average value of the Mulliken population as a function of the number of water molecules using the following function:

$$y = a(1 - \exp(bx)) + c \tag{21}$$

with $b < 0$.

If $n = 0$, then c is the gas-phase value when n goes to infinity, and the parameter a is equal to the difference between the fully solvated system and the gas phase. The nonlinear regression results are shown in Table 4. The predicted value of the Mulliken population for nitrogen in gas phase is 7.7547 ± 0.0088, in very good agreement with the calculated value for the gas phase (7.7474). The value for the saturated system is 7.9443 ± 0.0178 and corresponds to $n = 16$ (see Table 3 and Figure 3).

The chemical potential, i.e., the negative of the electronegativity, is in the frame of the frontier orbital theory equal to energy of the HOMO or the LUMO. From Figure 4a, we can see that e_{HOMO} decreases from −11.4 eV in gas phase to −12.4 eV for the cluster with one water. Addition of further water molecules increases the value of the left-side derivative to around −12.03 eV, with a standard deviation of 0.04 eV. It seems that this property does not change appreciably during solution. For e_{LUMO}, the predicted value for a saturated system is ∼7.0 eV (gas-phase value excluded in the correlation). The predicted value for $n = 0$ is 5.7790 ± 0.1177, the value for the direct gas-phase calculation being out of the error limit (6.13 eV). The results for the electrophilic, nucleophilic, and average chemical potential collected in Table 4 show a less satisfactory correlation with the proposed three parameter function. The

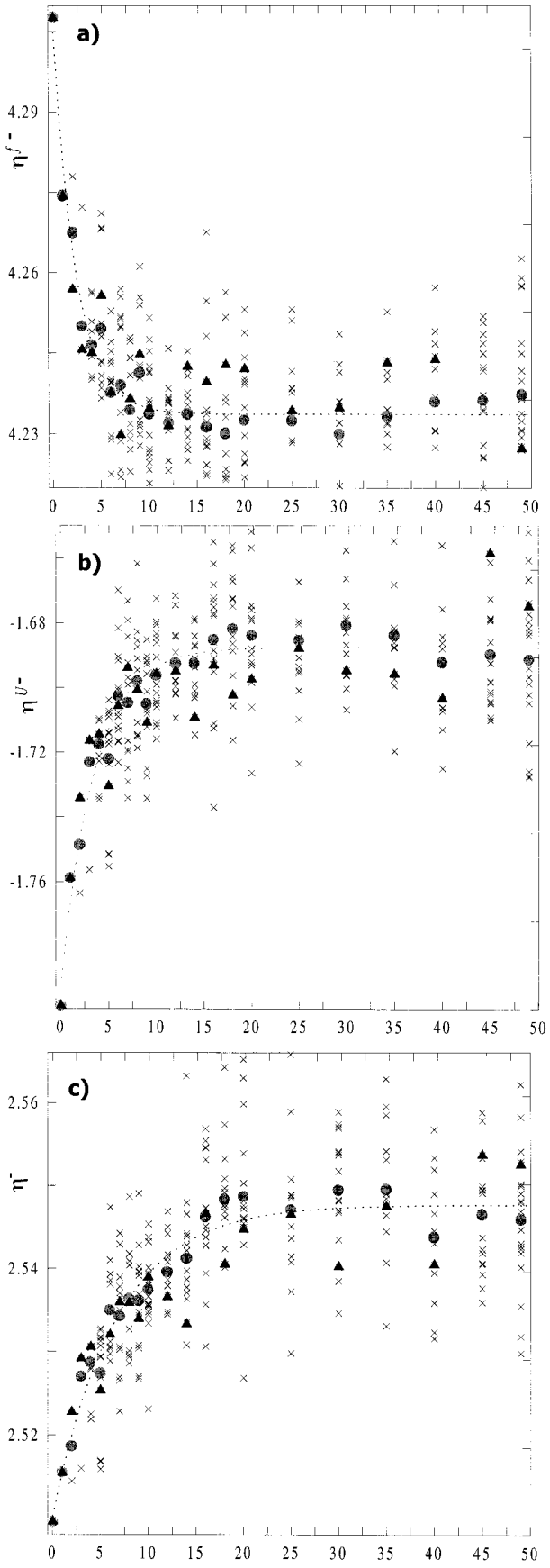

Figure 5. Electrophilic global hardness and its components for $NH_3(H_2O)_n$ as a function of the number of water molecules, n; (a) rigid part of the global hardness, η^{f-}; (b) relaxation part of the global hardness, η^{U-}; (c) electrophilic hardness, η, (all in eV). See Figure 3 for details.

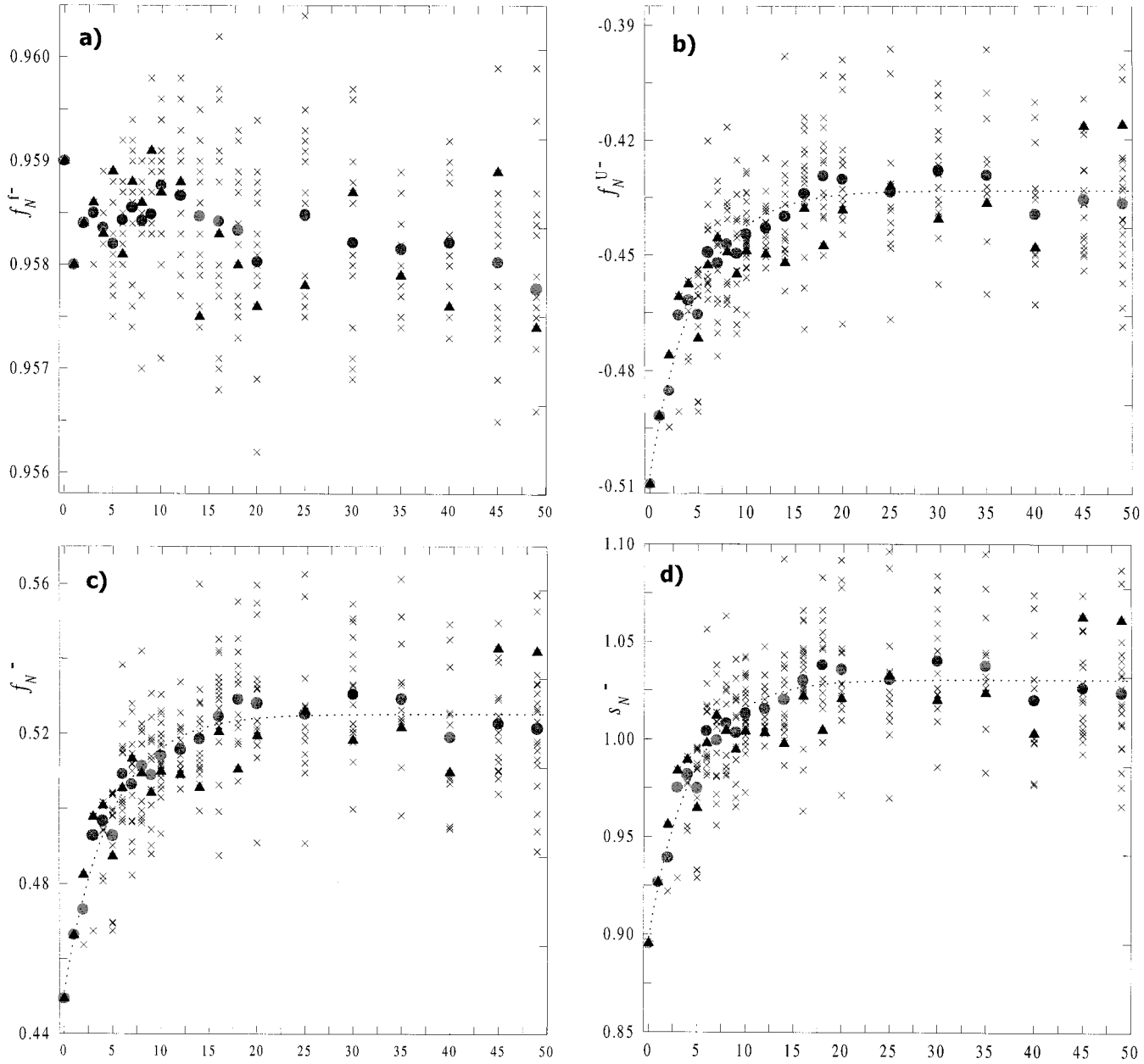

Figure 6. Condensed Fukui function and atomic softness for nitrogen atom in $NH_3(H_2O)_n$ as a function of the number of water molecule, n; (a) rigid part of FF, f^{f-}; (b) relaxation part of FF, f^{U-}; (c) condensed electrophilic FF, f^-; (d) electrophilic softness, s^- (in $10*eV^{-1}$). See Figure 3 for details.

nonlinear regression for Δ_{HL}, however, shows a very good correlation ($R^2 = 0.965$). The value for the saturated system is 9.5123 eV $\pm$ 0.0064, and just as for the Mulliken population, the gas phase value is very well reproduced (see Table 4.) This agrees perfectly with the work by Pearson, who studied changes in ionization energy (related to e_{HOMO}) and electron affinity (related to e_{LUMO}) upon solvation and noted that neutral molecules do not change their electronegativity (opposite of the chemical potential) while the HOMO−LUMO gap increases.[38]

The electrophilic hardness can be divided in two parts: a rigid part in which the coefficients of the wave function are "frozen" and only the occupation of the MO is changed (η^{f-}) and a part which represents the contribution from changes in the wave function coefficients (the relaxation part, η^{U-}). In Figure 5, we can see that the neglect of the relaxation contribution to the hardness can lead to erroneous conclusions. The rigid part of the hardness indeed decreases as a function of the number of water molecules (Figure 5a), and ammonia becomes softer in the solvent than in the gas phase. Addition of the relaxation part (Figure 5b), however, changes this trend completely, and the total electrophilic hardness increases with increasing number of water molecules (Figure 5c). The difference between the saturated value and the gas-phase values is, however, quite small, around 0.04 eV. The reason is that the hardness expression (eq 14) only contains two electron integrals and that there are no direct contributions from additional one electron terms in the Fock matrix. When the changes in the geometry are not so significant (the values of the one- and two-electron integrals in the AO basis are not changed) and there are no direct contributions from the **V** matrix, the solvent contribution in the hardness comes from modifications in the relaxation part, the **U** matrix (the difference between the **V** matrix in gas phase and solvent).

The atomic properties such as the electrophilic Fukui function and the atomic electrophilic softness for the nitrogen atom are presented in Figure 6. The analysis of the charge distribution

in the HOMO shows that the solvent hardly influences the rigid part of the condensed FF, the average value being 0.958 with a standard error of less than 10^{-4}. The relaxation part, however, has a significant influence on the final values of the electrophilic FF; the relaxation part increases from −0.509 for the gas phase to −0.433, the value predicted for the saturated system. Contributions from the relaxation part change the predicted values of the Fukui function for the saturated system from 0.959 for the rigid FF to 0.525 for the relaxed FF (∼40%). Generally, atomic FF and softness values increase with increasing number of water molecules. The point of saturation is similar to the Mulliken population located near $n = 16$. It is interesting that the global softness (inverse of the global hardness) decreases when the atomic softness of the nitrogen atom, a potential reactivity site, increases.

The values of the right-side derivatives (addition of an electron) for hardness show that the relaxation part for this quantity lowers the values by about 10%, as compared with those of rigid hardness. Similar to the left-side derivative for the chemical potential, the right-side derivative does not change appreciably from the value in the gas phase. The values of the condensed Fukui function for the nitrogen atom are negative value due to the "negative" population on the LU orbital; the reason for this may be the Mulliken population analysis scheme, which we adopted to evaluate the condensed FF. Continuum-model and full ab initio calculations (for one and two water molecules) also give negative values for the nitrogen's LU orbital population.

5. Conclusions

The effective fragment potential (EFP) model has been used to study the effect of adding increasing numbers of water molecules on several DFT-based reactivity descriptors of NH_3. The analysis of the incremental binding energy suggests that a sixteen water molecule ammonia cluster is energetically highly favored maximizing the number of O···HO hydrogen bonds and minimizing their deviation from an ideal linear orientation. The addition of water molecules increases the HOMO−LUMO gap and the electrophilic hardness. The importance of the relaxation part in the calculation of the solvent effect has been shown in the electrophilic hardness and the condensed Fukui function for the nitrogen atom. Increasing atomic softness for the nitrogen with decreasing of the global softness was observed. The saturation point for solvatation was located around a cluster with 16 water molecules fixing working conditions for systematic studies on solvatation of properties on (large) series of molecules. The evolution of the average values of atomic properties such as the nitrogen Mulliken population, condensed Fukui function, and atomic softness and global propertiessuch as the electrophilic hardness and its components with the number of water molecules shows an excellent fit with a three parameter exponential function. The atomic nucleophilic indices for the nitrogen atom show its high resistance against accepting electrons during nucleophilic reaction.

As a whole, the "chemistry" and internal consistency of the results of this study offer clear evidence that a combination of the CPHF and EFP model may be of optimal quality/cost for the systematic study on the solvent dependence of reactivity descriptors.

Acknowledgment. This work was supported by a research grant from the Flemish-Polish Scientific Cooperation Program. One of the authors (R.B.) also acknowledges NATO for a Research Fellowship. P.G. wishes to acknowledge the Free University of Brussels (VUB) for a generous computer grant and the FWO-Flanders for financial support. Helpful discussions with Dr. F. De Proft (VUB) and Dr. W. Bartkowiak (TUW) are gratefully acknowledged.

References and Notes

(1) See, for example: (a) Szafran, M.; Karelson, M. M.; Katritzky, A. R.; Koput, J.; Zerner, M. C. *J. Comput. Chem.* **1993**, *14*, 371. (b) Giesen, D. J.; Cramer, C. J.; Truhlar, D. G. *J. Phys. Chem.* **1995**, *99*, 7137. (c) Bianco, R.; Hynes, J. T. *J. Chem. Phys.* **1995**, *102*, 7864. (d) Tortonda, F. R.; Pascual-Ahuir, J. L.; Silla, E.; Tunon, I. *J. Phys. Chem.* **1995**, *99*, 12525. (e) Truong, T. N.; Stepanovich, E. V. *J. Chem. Phys.* **1995**, *103*, 3709. (f) Giesen, D. J.; Storer, J. W.; Cramer, C. J.; Truhlar, D. G. *J. Am. Chem. Soc.* **1995**, *117*, 1057.

(2) See, for example: (a) Warshel, A. *J. Phys. Chem.* **1979**, *83*, 1640. (b) Thole, B. T.; Van Duijnen, P. T. *Theor. Chim. Acta* **1980**, *55*, 307. (c) Thole, B. T.; Van Duijnen, P. T. *Chem. Phys.* **1982**, *71*, 211. (d) Singh, U. C.; Kollman, P. A. *J. Comput. Chem.* **1984**, *5*, 129. (e) Warshel, A.; King, G. *Chem. Phys. Lett.* **1985**, *121*, 124; (f) King, G.; Warshel, A. *J. Chem. Phys.* **1989**, *91*, 3647. (g) Field, M. J.; Bash, P. A.; Karplus, M. J. *J. Comput. Chem.* **1990**, *11*, 700. (h) Maseras, F.; Morokuma, K. *J. Comput.Chem.* **1995**, *16*, 1170.

(3) Day, P. N.; Jensen, J. H.; Gordon, M. S.; Webb, P.; Stevens, W. J.; Krauss, M.; Garmer, D. R.; Basch, H.; Cohen, D. *J. Chem. Phys.* **1996**, *105*, 1968.

(4) Freitag, M. A.; Gordon, M. S.; Jensen, J. H.; Stevens, W. J. *J. Chem. Phys.* **2000**, *112*, 7300.

(5) Wladkowski, B. D.; Krauss, M.; Stevens, W. J. *J. Am. Chem. Soc.* **1995**, *117*, 10537.

(6) Merrill, G. N.; Gordon, M. S. *J. Phys. Chem. A* **1998**, *102*, 2650.

(7) Chen, W.; Gordon, M. S. *J. Chem. Phys.* **1996**, *105*, 11081.

(8) Krauss, M.; Webb, S. P. *J. Chem. Phys.* **1997**, *107*, 5771.

(9) Day, P. N.; Pachter, R. *J. Chem. Phys.* **1997**, *107*, 2990.

(10) Peterson, C. P.; Gordon, M. S. *J. Phys. Chem. A* **1999**, *103*, 4166.

(11) Bandyopadhyay, P.; Gordon, M. S. *J. Chem. Phys.* **2000**, *113*, 1104.

(12) Parr, R. G.; Yang, W. *Density Functional Theory of Atoms and Molecules*; Oxford University Press: New York, 1989.

(13) Parr, R. G.; Yang, W. *Annu. Rev. Phys. Chem.* **1995**, *46*, 701.

(14) Geerlings, P.; De Proft, F.; Langenaeker, W. *Adv. Quantum Chem.* **1999**, *33*, 303.

(15) Chermette, H. *J. Comput. Chem.* **1999**, *20*, 129.

(16) Parr, R. G.; Donnelly, R. A.; Levy, M.; Palke, W. E. *J. Chem. Phys.* **1978**, *68*, 3801.

(17) Parr, R. G.; Pearson, R. G. *J. Am. Chem. Soc.* **1983**, *105*, 7512.

(18) Yang, W.; Parr, R. G.; *Proc. Natl. Acad. Sci. U.S.A.* **1984**, *82*, 6723.

(19) Parr, R. G.; Yang, W. *J. Am. Chem. Soc.* **1984**, *106*, 4049.

(20) Pearson, R. G. *J. Chem. Educ.* **1987**, *64*, 561.

(21) Sanderson, R. T. *J. Am. Chem. Soc.* **1952**, *74*, 272; *Science* **1951**, *114*, 670.

(22) Parr, R. G.; Pearson, R. G. *J. Am. Chem. Soc.* **1983**, *105*, 7512.

(23) Fukui, K. *Theory of Orientation and Stereoselection*; Springer-Verlag: Berlin, 1973.

(24) Geerlings, P.; De Proft, F. *Int. J. Quantum Chem.* **2000**, *80*, 227.

(25) De Proft, F.; Langenaeker, W.; Geerlings, P. *J. Phys. Chem.* **1993**, *97*, 1826.

(26) Safi, B.; Choho, K.; De Proft, F.; Geerlings, P. *J. Phys. Chem. A* **1998**, *102*, 5253.

(27) Safi, B.; Choho, K.; De Proft, F.; Geerlings, P. *Chem. Phys. Lett.* **1999**, *300*, 85.

(28) Safi, B.; Choho, K.; Geerlings, P. *J. Phys. Chem. A* **2001**, *105*, 591.

(29) Safi, B.; Balawender, R.; Geerlings, P. *J. Phys. Chem.*, submitted for publication.

(30) Balawender, R.; Komorowski, L. *J. Chem. Phys.* **1998**, *109*, 5203.

(31) Michalak, A.; De Proft, F.; Geerlings, P.; Nalewajski, R. *J. Phys. Chem. A* **1999**, *103*, 762.

(32) Balawender, R.; Geerlings, P. *J. Chem. Phys.* **2001**, *114*, 682.

(33) Balawender, R.; De Proft, F.; Geerlings, P. *J. Chem. Phys.* **2001**, *114*, 4441.

(34) Dunning, T. H., Jr.; Hay, P. J. In *Methods of Electronic Structure Theory*; Shaefer, H. F., III, Ed.; Plenum Press: New York, 1977; Chapter 1, pp 1−27.

(35) GAMESS: Schmidt, M. W.; Baldridge, K. K.; Boatz, J. A.; Elbert, S. T.; Gordon, M. S.; Jensen, J. J.; Koseki, S.; Matsunaga, N.; Nguyen, K. A.; Su, S.; Windus, T. L.; Dupuis, M.; Montgomery, J. A. *J. Comput. Chem.* **1993**, *14*, 1347.

(36) Geerlings, P.; Tariel, N.; Botrel, A.; Lissilour, R.; Mortier, W. J. *J. Phys. Chem.* **1984**, *88*, 5752.

(37) Gutman, V.; *The Donor Acceptor Approach to Molecular Interactions*; Plenum Press: New York, 1978.

(38) Pearson, R. G. *Chemical Hardness*; Wiley: New York, 1997.